Control of plasma fluctuations by using shaped ferromagnetic material

A. Komori,* K. Nishimura,† Y. Koide,‡ and N. Sato
Department of Electronic Engineering, Tohoku University, Sendai, Miyagi 980, Japan
(Received 31 January 1986; revised manuscript received 25 April 1986)

Measurements are performed in an attempt to control fluctuations of a collisionless magnetoplasma by using ferromagnetic material. A shaped ferromagnetic cylinder, which modifies an external uniform magnetic field to yield an $l=3$ helical configuration with magnetic shear, is realized and is set around the plasma column having drift-wave-type fluctuations. By increasing the region where the plasma column is surrounded by the ferromagnetic cylinder, the plasma fluctuations are demonstrated to be suppressed.

I. INTRODUCTION

There has been considerable interest in simple methods to stabilize energetic plasmas in magnetic containment devices. A helical magnetic configuration with magnetic shear is well known[1,2] to have a stabilizing effect on plasma instabilities. It is, however, often pointed out that a set of helical windings necessary for this configuration is complicated to construct. Sheffield[3] has proposed using ferromagnetic materials which are shaped to provide helical magnetic field configurations instead of the complicated helical windings. It was shown theoretically that an $l=3$ helical stabilizer formed by six iron bars has a stabilizing effect on plasma fluctuations in a magnetic field below 10 kG. This idea has been further extended by Ikuta and Hirano.[4] But there has been no experimental confirmation of this method as being useful for plasma stabilization. Here a shaped ferromagnetic cylinder is manufactured to yield an $l=3$ helical magnetic configuration with magnetic shear and is demonstrated to be useful for suppression of plasma fluctuations.

II. EXPERIMENTAL APPARATUS

The experiment was performed on a collisionless magnetized plasma column. The potassium plasma of 3.5 cm in diameter was produced in a single-ended Q machine under an electron-rich condition,[5] as shown in Fig. 1. The plasma density n_0 was in the range 10^8–10^9 cm^{-3}. The electron temperature T_e was approximately equal to the hot-plate temperature (2000–2500 K), and the ion temperature $T_i \lesssim T_e$. The plasma was terminated by a movable 7-cm-diam endplate which could be biased to draw axial electron currents. A ferromagnetic cylinder of 150 cm length was set inside the vacuum chamber of 15.6 cm diameter to surround the plasma column (see Fig. 1). The cylinder was movable in the axial (z) direction along the externally applied magnetic field B_0, which could be varied up to 4 kG. The background gas pressure was kept less than 2×10^{-6} Torr. Small movable Langmuir probes, which can also work as emissive probes,[6] were used to measure the plasma parameters and their fluctuations.

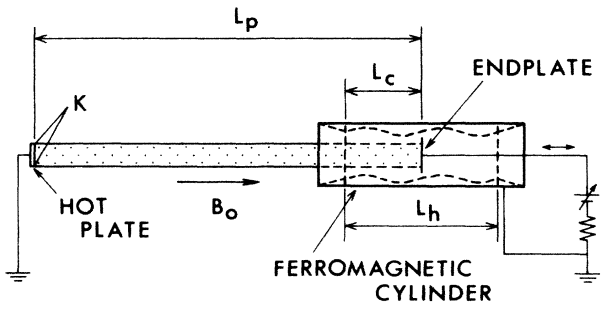

FIG. 1. Schematic of experimental apparatus.

A main part of the ferromagnetic cylinder, whose length L_h is 110 cm, consists of 180 soft iron rings shown in Fig. 2(a). The thickness and outer radius of the rings are 0.61 and 4.8 cm, respectively. The inner shape of the rings is described by

$$r=r_0[1+\epsilon\sin(3\theta)]\ ,$$

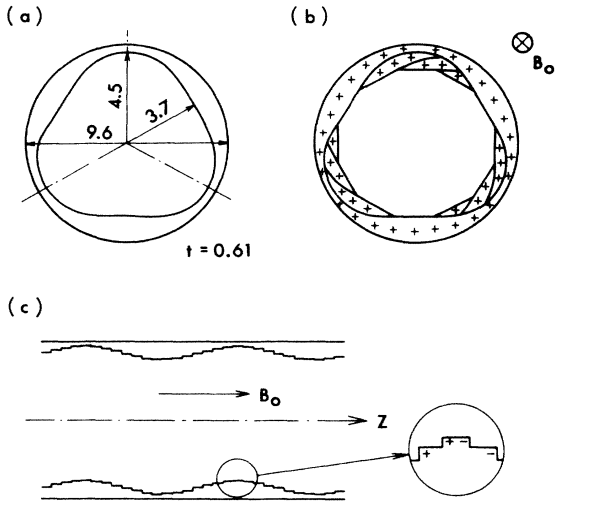

FIG. 2. A ferromagnetic cylinder is formed by using 180 soft iron rings as shown in (a). The thickness of the rings is 0.61 cm. They are placed axially in a row but are rotated little by little azimuthally as shown in (b) and (c). Magnetic charges appear on the surfaces perpendicular to the externally applied magnetic field B_0, as also shown in (b) and (c).

where r is the radial position, θ is the azimuthal angle, $r_0=4.1$ cm, and $\epsilon=0.1$. The saturation magnetization was 16.1 kG. The cylinder was formed by placing these rings closely in a row with their axes on the same line but by rotating each ring little by little azimuthally in the same direction [see Fig. 2(b)] so that the inner wall of the cylinder could be approximated by

$$r=r_0[1+\epsilon\sin(3\theta-kz)] .$$

When the ferromagnetic cylinder formed is set with its axis along the external magnetic field [see Figs. 1 and 2(c)], magnetic charges with helical symmetry are induced on the wall surfaces perpendicular to B_0, as shown in Figs. 2(b) and 2(c). These magnetic charges yield a helical magnetic configuration, with $l=3$ in this case, which is usually generated by electron currents in the external helical windings. Detailed calculations for the helical field can be found in Ref. 4. In our case, k was chosen to be 0.69 cm^{-1}, for which the azimuthal magnetic field formed is expected to have a maximum value. Different soft iron rings of 20 cm length were added to both ends of this main part of the cylinder in order to suppress the change of the magnetic field at the edges of the cylinder. These rings have a circular cross section, as shown in Fig. 3(a); the outer radius is 4.8 cm, and the inner radius becomes small from 4.6 to 4.1 cm toward the rings for the helical configuration. If these additional rings are not used, lots of magnetic charges are induced on the end surfaces perpendicular to B_0, and modify the external magnetic field intensively. The additional rings make this change of the magnetic field small, as shown in Fig. 3(b), since the magnetic charges are dispersed on their oblique surfaces.

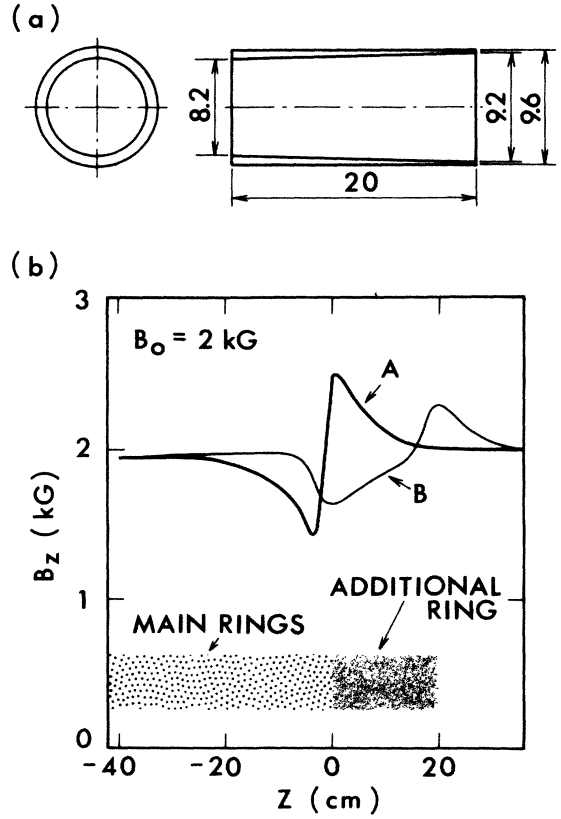

FIG. 3. (a) An additional soft iron ring which is added to both ends of the main part of the ferromagnetic cylinder for the helical configuration. (b) Axial magnetic fields B_z on the z axis ($r=0$), measured at the edge of the cylinder. The A and B are obtained without and with the additional ring, respectively. Ring locations are shown in the figure.

III. EXPERIMENTAL RESULTS AND DISCUSSION

Figure 4 shows the rotational transform angle ι provided by our ferromagnetic cylinder at $B_0=2$ kG as a function of radial position r, together with the corresponding shear length L_s $[=(180/\pi)(L_h/r)/(d\iota/dr)]$. The angle ι is measured by using an electron gun and a movable fluorescent plate which yields light emission if the electron beam collides with it. It can be seen from Fig. 4 that ι is zero on the z axis and increases (thus L_s decreases) with an increase in r. This is typical of the usual $l=3$ helical magnetic field.[7] L_s was found to be about 200 cm at the plasma edge ($r\cong 1.75$ cm). To compare the measured results with theoretical values, we used the magnetic scalar potential ϕ_m given by[8]

$$\phi_m=-B_0z+\frac{1}{4\pi}\int\frac{\mathbf{n}\cdot\mathbf{M}}{R}dS ,$$

where $\mathbf{M}$ is the magnetizing vector, $\mathbf{n}$ is the unit normal vector of the surface element dS, and R is a distance between the surface element and a measuring point. The rotational transform angle and the shear length are obtained from the axial, radial, and azimuthal components of the magnetic field B $(=-\nabla\phi_m)$. In the calculation, self-magnetization effects are taken into account. In Fig. 4, the calculated values are found to be consistent with the measured values.

The ferromagnetic cylinder mentioned above is now set in the vacuum chamber under the uniform external mag-

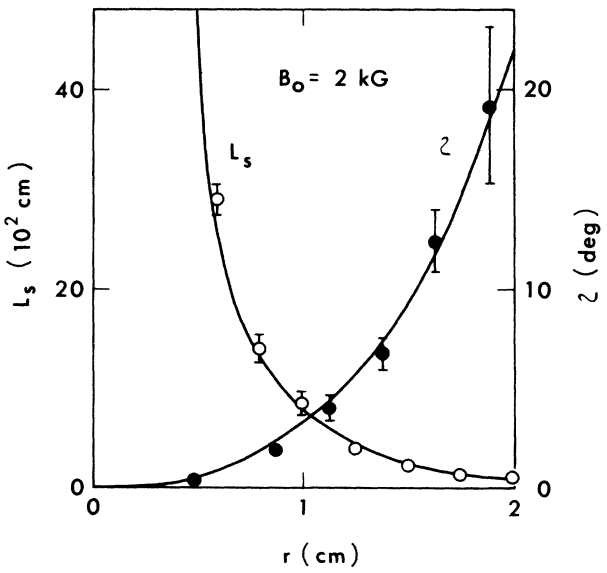

FIG. 4. Rotational transform angle ι and shear length L_s as a function of radial position r. Solid lines denote theoretical values.

netic field. At first the endplate is situated in front of the cylinder (and thus there is no plasma in the cylinder) in order to investigate the property of the plasma under the uniform magnetic field. Ion-current fluctuations displayed on a spectrum analyzer show that there are quite small fluctuations generated spontaneously in the plasma. To find a noticeable difference between the fluctuation levels with and without the ferromagnetic cylinder, large-amplitude plasma fluctuations are generated by biasing the endplate to drive an axial electron current.[9] Even if the axial current is small, the fluctuations are observed to be enhanced and to grow with an increase in the current. A typical spectrum is shown in the uppermost trace in Fig. 5. Here, L_c and u_d represent the length of the plasma column which is surrounded by the sheared magnetic field, and the electron drift velocity which is estimated from measurements of radial density profiles and currents flowing into the endplate I_e ($u_d = I_e/e\int n_0 dS$), respectively. At $u_d/v_e \cong 0.01$ (v_e is the electron thermal speed), the percentage fluctuation $\tilde{n}/n_0$ is measured to be about 10% at the position of the peak amplitude. This peak at $r \cong 1$ cm is located at a radial position of the maximum density gradient on the plasma cross section. The fluctuations propagate azimuthally, with mode numbers $m = 1,2,3,\ldots$, in the direction of electron diamagnetic drift, which coincides with that of $\mathbf{E}_0 \times \mathbf{B}_0$ drift ($\mathbf{E}_0$ is the radial electric field). The phase difference between the fluctuations of density and potential is obtained by the two probes located 45° apart azimuthally at $r = 1$ cm. One is used to obtain the reference signal, that is, the perturbed ion-saturation current $\tilde{J}_i$(ref). Another is used as the cold Langmuir probe and electron emissive probe to measure the fluctuations of ion-saturation current $\tilde{J}_i$ and potential $\tilde{\phi}_s$, respectively. A comparison of the phase difference between $\tilde{J}_i$ and $\tilde{J}_i$(ref) and the phase difference between $\tilde{\phi}_s$ and $\tilde{J}_i$(ref) shows that the density fluctuation leads the potential fluctuation by approximately 60°. There is no appreciable axial phase change of $\tilde{J}_i$. All these features of the fluctuations observed are reasonable for the collisionless drift-wave instability driven by the axial electron current.[9]

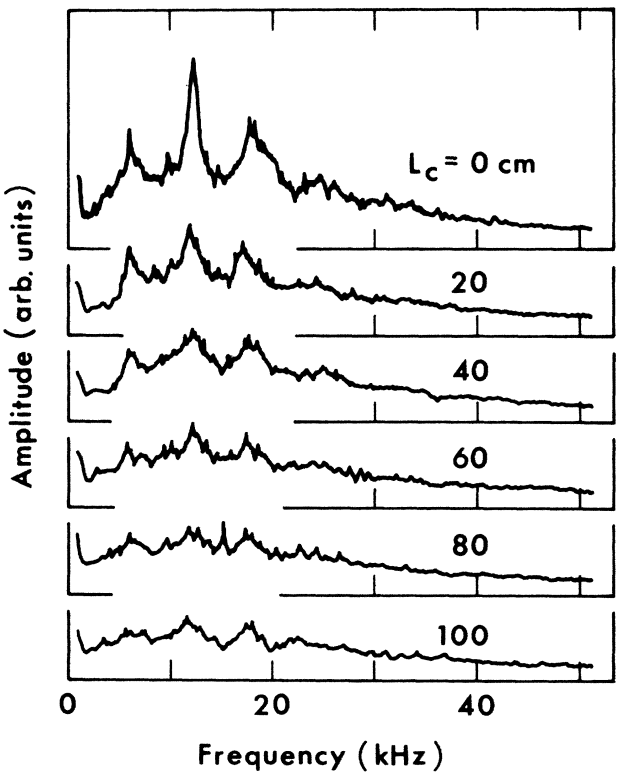

FIG. 5. Dependence of frequency spectrum on L_c. L_p is changed from 110 to 210 cm as L_c increases from 0 to 100 cm. Normalized electron flow speed $u_d/v_e \cong 0.01$ (v_e is the electron thermal speed).

By pulling out the endplate along the z axis, the plasma column is guided into the region of the ferromagnetic cylinder. Then we can observe a clear change of the frequency spectrum as shown in Fig. 5. Here the fluctuations are measured in the uniform region of the magnetic field because there is no appreciable change of the fluctuations along the plasma column. The fluctuation level decreases when we increase the region (L_c in Fig. 1) where the plasma is surrounded by the sheared field. At $L_c \cong 100$ cm, the instability is found to be extremely suppressed. By moving the endplate, however, both L_c and L_p (plasma length) are changed. When we push the ferromagnetic cylinder toward the hot plate, L_c is increased with no change in L_p. By increasing L_c at a fixed value of L_p in this way, the fluctuation level is observed to be also reduced. The measurements show that the fluctuation amplitude becomes small with a decrease in the effective shear length L_{se} ($= L_s L_p / L_c$). At $L_{se} \cong 500$ cm, the fluctuation level is found to be smaller by an order of magnitude than that at $L_{se} = \infty$.

Under a sheared magnetic field, the axial wave number k_z of drift waves is known[10,11] to be given by $k_z = k_{z0} + k_y \Delta r / L_s$, where k_{z0} is the axial wave number in the absence of the magnetic shear, k_y is the azimuthal wave number, and Δr is the radial width of the waves. The second term on the right-hand side of this equation indicates an increase in k_z in the presence of the magnetic shear, being responsible for the suppression of drift-wave instability. In our case, the plasma column is partly surrounded by the sheared magnetic field. And the measured results can be understood by taking account of the effective shear length L_{se} instead of L_s. A detailed comparison of the results with theoretical prediction will be published elsewhere.

IV. CONCLUSION

We have made a shaped ferromagnetic cylinder to form an $l = 3$ helical magnetic configuration with magnetic shear and demonstrated a suppression of drift-wave instability by using the ferromagnetic cylinder. Our work suggests that the method of using ferromagnetic materials might be applied to various magnetic plasma containment devices if the ferromagnetic materials would be shaped appropriately.

ACKNOWLEDGMENTS

We would like to thank Dr. K. Ikuta for his fruitful discussions. We are also indebted to H. Ishida and Y. Takahashi for their technical assistance.

*Present address: Interdisciplinary Graduate School of Engineering Sciences, Kyushu University, Kasuga 816, Japan.
†Present address: Institute of Plasma Physics, Nagoya University, Nagoya 464, Japan.
‡Present address: Division of Thermonuclear Fusion Research, Japan Atomic Energy Research Institute, Tokai-mura, Naka-gun, Ibaraki 319-11, Japan.

[1]L. Spitzer, Phys. Fluids **1**, 253 (1958); F. F. Chen and D. Mosher, Phys. Rev. Lett. **18**, 639 (1967); P. E. Scott, P. F. Little, and J. Burt, *ibid.* **25**, 996 (1970).
[2]A. Komori, N. Sato, and Y. Hatta, Phys. Rev. Lett. **40**, 768 (1978).
[3]G. Sheffield, Princeton University Plasma Physics Laboratory Report No. MATT-721, 1969 (unpublished).
[4]K. Ikuta and K. Hirano, Nucl. Fusion **20**, 35 (1980).
[5]N. Sato, H. Sugai, and R. Hatakeyama, Phys. Rev. Lett. **34**, 931 (1975).
[6]R. F. Kemp and J. M. Sellen, Jr., Rev. Sci. Instrum. **37**, 455 (1966).
[7]K. Miyamoto, Nucl. Fusion **18**, 2 (1978).
[8]J. A. Stratton, *Electromagnetic Theory* (McGraw-Hill, New York, 1942).
[9]J. J. Thomson, G. Benford, N. Rynn, and W. S. Williamson, Phys. Fluids **17**, 1008 (1974); R. Hatakeyama, M. Oertl, E. Märk, and R. Schrittwieser, *ibid.* **23**, 1774 (1980).
[10]F. F. Chen, Phys. Fluids **9**, 965 (1966).
[11]A. Komori and N. Sato, Jpn. J. Appl. Phys. **23**, 475 (1984).

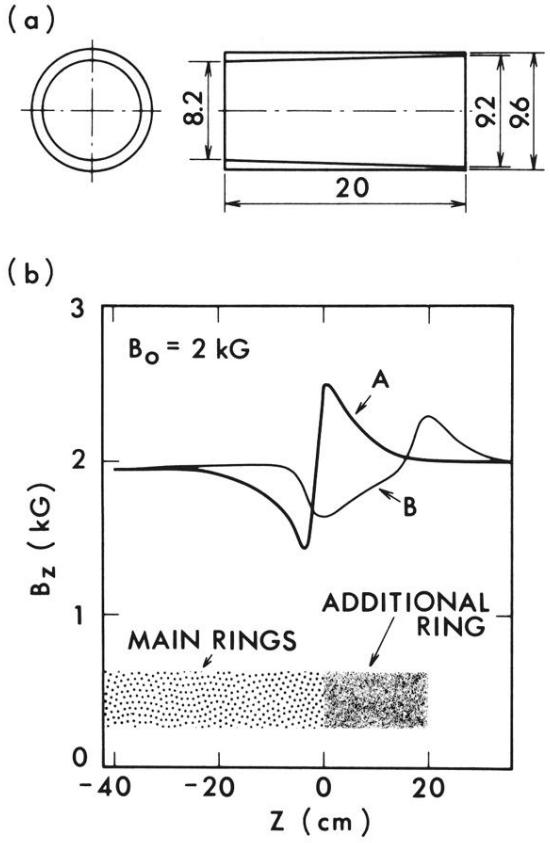

FIG. 3. (a) An additional soft iron ring which is added to both ends of the main part of the ferromagnetic cylinder for the helical configuration. (b) Axial magnetic fields B_z on the z axis ($r=0$), measured at the edge of the cylinder. The A and B are obtained without and with the additional ring, respectively. Ring locations are shown in the figure.